Sigma Journal of Engineering and Natural Sciences
Web page info: https://sigma.yildiz.edu.tr
DOI: 10.14744/sigma.2022.00041

Research Article

Design and optimization of impact attenuator for a Formula SAE racing car

Doğukan KAYA[1], Erdem ÖZYURT[1]*

[1]*Eskisehir Technical University, Department of Mechanical Engineering, 26555, Eskisehir, Turkey*

ARTICLE INFO

Article history
Received: 14 December 2020
Accepted: 13 April 2021

Key words:
Energy absorption; Formula SAE; Impact Attenuator; Frontal Collision; FEM

ABSTRACT

Impact attenuators are passive safety components that are developed to protect the structural elements of the vehicle and the people inside it. In this study, an impact attenuator is designed for Formula SAE (Society of Automotive Engineering) competition racing car. Due to the SAE regulations, the impact attenuator must absorb 7350 J of collision energy in a frontal collision at a speed of 7 m/s, without resulting in any deformation to the vehicle structural elements. Numerical simulations are performed using ANSYS Workbench finite element software. The material model for the impact attenuator is selected as AA6061-T6 aluminum alloy due to its high energy absorption performance. It is found that the design with varying wall thickness to be the most efficient in terms of crash force efficiency and specific energy absorption when compared to the basic conical impact attenuator design. A reduction of 64.99% on the maximum impact force, an increase of 58.76% deformation, and an increase of 30.77% crash force efficiency were achieved between the first design and the final design with varying thickness.

Cite this article as: Doğukan K, Erdem Ö. Design and optimization of impact attenuator for a Formula SAE racing car. Sigma J Eng Nat Sci 2022;40(2):390-401.

INTRODUCTION

The safety of passengers and drivers in a vehicle is one of the highest responsibilities of automotive manufacturers. Accidents always occur either caused by the driver or external factors. By observing these accidents, the German Insurance Association (GIA) carried out statistical evaluations of collisions where cars were damaged or passengers were injured; 79% of the accidents were due to the mistakes made by the drivers, the remaining 21% were due to the road, weather conditions, etc. [1]. Thus, manufacturers and researchers developed active and passive safety systems that ensure the safety of both vehicles and the occupants. Impact attenuators are one of the passive safety systems that ensure the integrity of structural elements of the vehicle and the safety of the passengers in the event of an accident. Especially for a racing car traveling at high speeds, fatal consequences may occur for the driver in case of an

***Corresponding author.**
*E-mail address: eozyurt@eskisehir.edu.tr

This paper was recommended for publication in revised form by Regional Editor Hasan Koten

Sigma J Eng Nat Sci, Vol. 40, No. 2, pp. 390–401, June, 2022

accident. Due to the relatively high speed of the race car, a high amount of impact energy is released in case of a frontal collision. Therefore, the impact energy must be absorbed by an impact attenuator located at the frontal bulkhead of the racing car.

Crashworthiness defines the energy absorbing capability of the vehicle in a collision. Energy absorbing elements mostly rely on structural fractures, buckling, and plastic deformation to absorb the impact energy [2, 3]. Sufficient crashworthiness of the racing car is an expected criterion for the safety of the driver in the event regulations of the Formula SAE competition. An impact attenuator must be installed on the frontal bulkhead of the race car. By the Formula SAE regulations, impact attenuator mounted in the frontal bulkhead must satisfy the following requirements [4]:

a. At least 200 mm long, with its length oriented along the fore/aft axis of the frame.
b. At least 100 mm vertically (perpendicular to the ground) and 200 mm laterally (parallel to the ground) for a minimum distance of 200 mm forward of the Front Bulkhead.
c. Designed impact attenuator must not be penetrating the front bulkhead in the event of a collision.
d. When an impact attenuator mounted on the front of a racing car with a total mass of 300 kg, and run into a solid, non-yielding impact barrier at a velocity of 7 m/s, the impact attenuator must be absorbing all the 7350 J impact energy or more of the energy will be released in a frontal collision. Also, the average deceleration of the racing car should not exceed 20 g, with a peak deceleration less than or equal to 40 g.

There are no rules other than the specified criteria, and the originality in design is left to the contestants. Also, the material to be used for the impact attenuator is not restricted by the rules, contestants are free to choose any type of material. In energy absorption studies, aluminum alloy is a widely preferred material because it is lightweight, cheap, and easily accessible. In the existing literature, it was proven that aluminum alloy is a good choice of material due to its energy absorption capacity [5-7]. It was also used in both low-velocity [8] and high-velocity [9] impact application studies.

The shapes of deformable impact attenuators include steel drums [10], circular tubes [11], tubular rings [12], square tubes [13], corrugated tubes [14], multi-corner columns [15], frusta [16], struts [17], honeycomb cells [18], sandwich plates [19] and some other particular shapes such as stepped circular thin-walled tubes [20] and top-hat thin-walled sections [21]. However, from the evidence in many studies in the literature, thin-walled conical impact attenuators with circular cross-sections are preferred due to their energy absorption efficiency and ease of manufacture [22, 23]. Belingardi et al. [24], showed that circular and elliptical holes on the thin-walled frustum impact attenuators have a better energy absorption efficiency, and improves specific energy absorption (SEA) because of their lightweight.

The response of thin-walled impact attenuators to axial impact depends on several parameters. One of which is the geometrical parameters such as length, width, and thickness, which directly influence the deformation shape of the impact attenuator. In a numerical study of thin-walled impact attenuators, Jensen et al. [25] proved that the transition from progressive to global buckling is highly dependent on the impact velocity. Considering the energy absorption efficiency, the desired deformation type of the impact attenuators is local buckling [26-28].

This study aims to design an impact attenuator to prevent the deformation of the structural components of the Formula type single-seater race car that will participate in the race within the scope of the Formula SAE competition. Although there is a sufficient number of academic publications on the subject of energy absorption since the subject is related to safety, it is constantly being worked on and development studies continue in this area. The difference between this study from existing studies is that it is designed for a special type of vehicle and includes the optimization of the energy absorber that will meet certain regulations. For this purpose, various design parameters were numerically investigated for the particular case. Equations and brief information about energy absorption phenomena were presented. Results and discussion sections were given including the optimized geometry. Finally, the conclusions based on findings were provided.

DEFINITIONS OF ENERGY ABSORPTION CONCEPT AND DEFORMATION

In the event of a collision, the kinetic energy of the racing car is transformed into the impact energy which the impact attenuator absorbs through plastic deformation. Impact attenuators are expected to be able to absorb large amounts of energy, but this energy absorption also has a limit. During the collision, the impact forces on the surface struck by the impact attenuator must have a maximum limit value depending on the material properties of the impact attenuator. Otherwise, catastrophic failure occurs if this maximum limit value is exceeded.

Total energy absorption is defined as the work done by impact force. The total energy absorption is expressed as:

$$E_t = \int F_{impact} \cdot d\delta \tag{1}$$

where E_t is the total energy absorption, F_{impact} is the impact force, and δ is the deformation. Also, the same equation expressed by an average impact force and deformation.

$$E_t = \int_{\delta_p}^{\delta} F_{impact,ave} \cdot d\delta = F_{impact,ave} \cdot \left(\delta - \delta_p\right) \tag{2}$$

where $\delta - \delta_p$ is the deformation range and $F_{impact,ave}$ is the average impact force obtained as:

$$F_{impact,ave} = \frac{E_t}{\delta_t} \tag{3}$$

where E_t is the total energy absorption and δ_t is the total deformation. In addition to total energy absorption, specific energy absorption should be taken into consideration depending on the amount of energy absorbed and the weight of the impact attenuator. The specific energy absorption (SEA) can be expressed as:

$$E_{SEA} = \frac{E_t}{m} \tag{4}$$

where E_{SEA} is the specific energy absorption (SEA), E_t is the total energy absorption, and m is the mass of the impact attenuator. The designed impact attenuator should be as light as possible. Weight is an important factor in the impact attenuator to keep the vehicle balanced and maintain the center of gravity. This factor may differ depending on the vehicle's weight. The impact attenuator used in automobiles is desired to be light, but the lightness of the impact attenuator used in high tonnage trucks is not of great importance.

The crash force efficiency (CFE) is expressed as:

$$CFE = \frac{F_{impact,ave}}{F_{max}} \tag{5}$$

where is *CFE* the crash force efficiency, $F_{impact,ave}$ is the average impact force, and F_{max} is the maximum impact force response of the impact attenuator.

Since collision analysis contains complicated calculations, numerical methods are used. Among the large number of software on such type of analysis, ANSYS Workbench is one of the most widely used. [29, 30] For this reason, the study was conducted with ANSYS Workbench. There are two methods of time integration used in ANSYS Workbench; implicit and explicit. In the implicit time integration method, displacement is not the function of time. Therefore, the calculation is carried out by neglecting the velocity and acceleration values obtained by the derivatives of displacement. This method is not suitable for cases caused by large deformations and where high speeds are reached in a short time. Unlike implicit methods, the explicit method is time-dependent. Therefore, velocity, acceleration, mass, and damping are considered with this method. Hence, the main method used in the present study is the explicit finite element analysis, which is known to be a better method for structural problems involving large deformations, high strain rates, and complex contact interactions occurring within a short amount of time. [31, 32]

The central differences method is used for the integration of motion equations in ANSYS Workbench / Explicit Dynamics software. In the central differences method, the position, velocity-acceleration expressions in the equation of motion are written to include the previous and next time steps. The equations of motion of the system are solved by placing these time-dependent expressions and the derivative of position with respect to time into the equation of motion of the system.

A dynamic system can be mathematically expressed by ordinary differential equations. The equation of motion of the system includes displacement (position), velocity, and acceleration. Velocity and acceleration are expressed in time derivatives of position. Velocity and acceleration equations are shown in 6 and 7:

$$\dot{u}_n = \frac{1}{2 \cdot \Delta t} \cdot \left(u_{n+1} - u_{n-1} \right) \tag{6}$$

$$\ddot{u}_n = \frac{1}{(\Delta t)^2} \cdot \left(u_{n+1} - 2u_n + u_{n-1} \right) \tag{7}$$

where n, $n + 1$ and $n - 1$ subscripts represent the current (t_n), one step next (t_{n+1}) and one step earlier (t_{n-1}) system states, respectively.

The equation of motion of the system at the time t_n expressed as:

$$\boldsymbol{M}\ddot{u}_n + \boldsymbol{C}\dot{u}_n + \boldsymbol{K}u_n = \boldsymbol{P}_n \tag{8}$$

where $\boldsymbol{M}$ is the mass matrix, $\boldsymbol{C}$ is the damping matrix, $\boldsymbol{K}$ is the rigidity matrix and $\boldsymbol{P}_n$ is the external loading matrix.

$$\left(\boldsymbol{M} + \frac{1}{2}\Delta t \cdot \boldsymbol{C} \right) u_{n+1} = \Delta t^2 \cdot \boldsymbol{P}_n - \left(\Delta t^2 \cdot \boldsymbol{K} - 2\boldsymbol{M} \right) u_n - \left(\boldsymbol{M} - \frac{\Delta t}{2} \cdot \boldsymbol{C} \right) u_{n-1} \tag{9}$$

Finally, if the displacement, velocity, and acceleration expressions are written in equation 8, the equation of motion for the system is obtained as in Equation 9.

Deformation Modes

Impact attenuators absorb the impact energy by plastic deformation. The plastic deformation pattern formed in the impact attenuators differs according to the type of loading. Generally, three deformation types that exist for impact attenuators are global buckling, local buckling, and catastrophic failure (sudden load-bearing capacity loss). However, a catastrophic failure is undesirable for an impact attenuator design.

Global buckling is referred to as Euler's buckling. This type of deformation reduces the energy absorption capability of a structure, so it is an undesirable form of buckling in energy absorption applications [26]. However, local

Sigma J Eng Nat Sci, Vol. 40, No. 2, pp. 390–401, June, 2022

buckling is the desirable form of deformation for impact attenuators because only axial forces occur on the impact attenuator. This causes the impact attenuator to deform with the folds spread at certain intervals close to a homogeneous distribution [33].

MATERIALS AND METHODS

The main method used in the present study is the explicit finite element analysis, which is known to be better in comparison to the implicit method for structural problems involving large deformations, high strain rates, and complex contact interactions occurring within a short amount of time [31, 32]. In this study, the commercial finite element program ANSYS Workbench/Explicit Dynamics was used for simulating the behavior of the impact attenuator system during the collision of the race car.

Numerical Model

The measurements of all impact attenuators analyzed in the study were designed in accordance with the Formula SAE regulations. The detailed model drawings are shown in Figure 1 and the dimensions of the designs are given in Table 1.

Initial and Boundary Conditions

The initial and boundary conditions defined in the finite element model must reflect the actual real-life condition of the collision so that the response of the impact attenuator can be correctly predicted. In this analysis, the impact attenuator and the race car have an initial velocity of 7 m/s as mentioned in the Formula SAE regulations.

There are three main parts in the geometric assembly. These are the impact attenuator, the rigid wall, and the base part which represents the race car. The impact attenuator and base part were bonded together during the

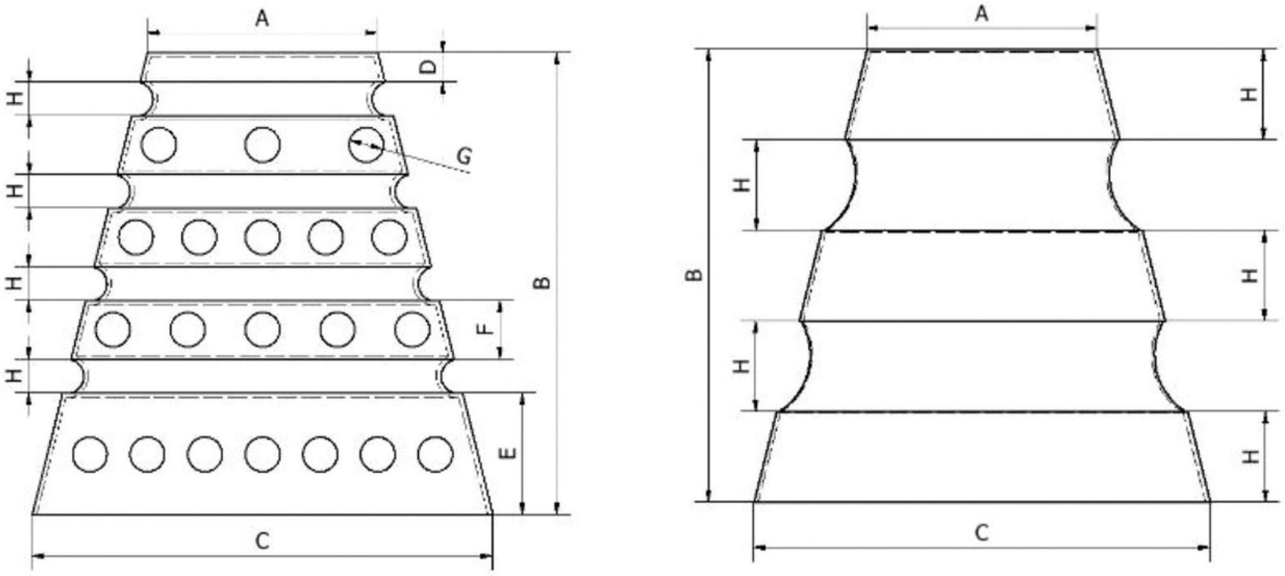

Figure 1. Dimension details of impact attenuator designs.

Table 1. Dimensions of all impact attenuators.

Dimensions	2 mm	2 mm with grooves	2 mm with grooves and holes	varying thickness with grooves
A [mm]	100	100	100	100
B [mm]	200	200	200	200
C [mm]	200	200	200	200
D [mm]	-	12.72	12.72	-
E [mm]	-	52.72	52.72	-
F [mm]	-	25.45	25.45	-
G [mm]	-	-	15	-
H [mm]	-	14.55	14.55	40

collision. The contact between the impact attenuator and the rigid wall was set as frictional contact pair with kinematic and dynamic frictional coefficients of 0.2 and 0.1 respectively which is also commonly used in the current literature [34].

The displacement of the rigid wall in which the impact attenuator crashes was restricted in all axes. Therefore, when the impact attenuator collides with the rigid wall, the wall has to stand still at its position. The base part and impact attenuator can translate only in the direction of movement. For better visualization of the analyzed model, the collision model is shown in Figure 2.

Material Selection

The choice of material model is very important as it directly affects the energy-absorbing behavior of the part. The preferred material in this study is aluminum alloy AA6061-T6 due to its reputation with energy absorption performance [9, 35]. This material was coupled with Johnson-Cook constitutive material model to consider the effect of the velocity on the deformation. The material properties for Aluminum alloy AA6061-T6 provided by Lesuer et al. [35] are given in Table 2.

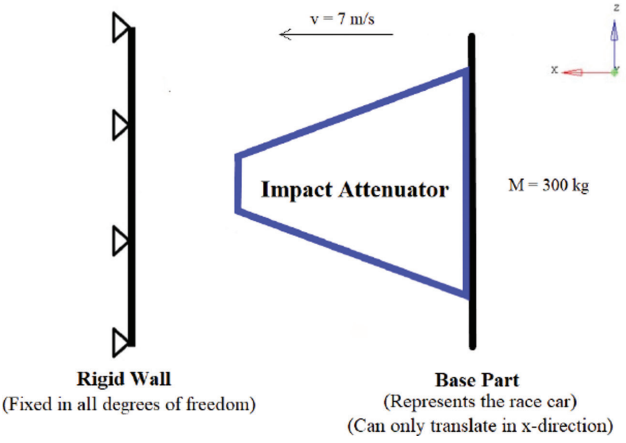

Figure 2. Collision model of the Impact Attenuator.

The material of the base part and a rigid wall was selected as structural steel. The material properties of structural steel are taken from the material library of the ANSYS Workbench software and the corresponding properties are shown in Table 3.

Mesh Modeling

The mesh method should be properly selected depending on the geometry of the design. According to the structure of the geometry, a multizone method was selected for meshing operations. Since the number of elements depends on the element length, operations can be performed by changing the element length adjustments on the software. As the element size gets smaller, the analysis gives more accurate results, but the analysis time increases significantly. For this reason, it is very important to determine the optimum element size. There are quality criteria in ANSYS Workbench to determine these optimum values, which are:

Element Quality: It shows on a 0 to 1 quality scale according to the result of the analysis. A minimum of 0.7 quality elements gives efficient results for analysis [36].

Skewness: Indicates the distortions / irregularities of triangles and rectangles formed in the mesh according to the internal angles. In the scale given between 0 and 1, it gives optimum results when the values approach 0 [36].

Aspect Ratio: For the triangles and quadrilaterals in the mesh, the best view indicates the function of the ratio of the longest edge of the reconstructed quadruple to the shortest edge. The fact that the values are close to 1 indicates that the results are efficient [36].

Using these criteria, a mesh optimization study has been carried out and the optimum element length has been selected as 3 mm. The trials and results of the given element quality criteria are given in Table 4. The detailed meshing of the design is shown in Figure 3.

a. 2 mm thick square cross-sectioned,
b. 2 mm thick circular cross-sectioned,
c. 2 mm with grooves
d. 2 mm with grooves and holes
e. varying thickness with grooves

Table 2. The material properties and Johnson-Cook constants for AA6061-T6 [35].

E [GPa]	σ_y [MPa]	E_t [MPa]	ρ [kg/m³]	v [-]	A [MPa]	B [MPa]	n	C	m
70	276	562	2700	0.33	324	114	0.42	0.002	1.34

Table 3. The mechanical properties of structural steel.

Material	E [MPa]	σ_y [MPa]	ρ [kg/m³]	v [-]
Structural Steel	200 000	250	7850	0.30

Sigma J Eng Nat Sci, Vol. 40, No. 2, pp. 390–401, June, 2022

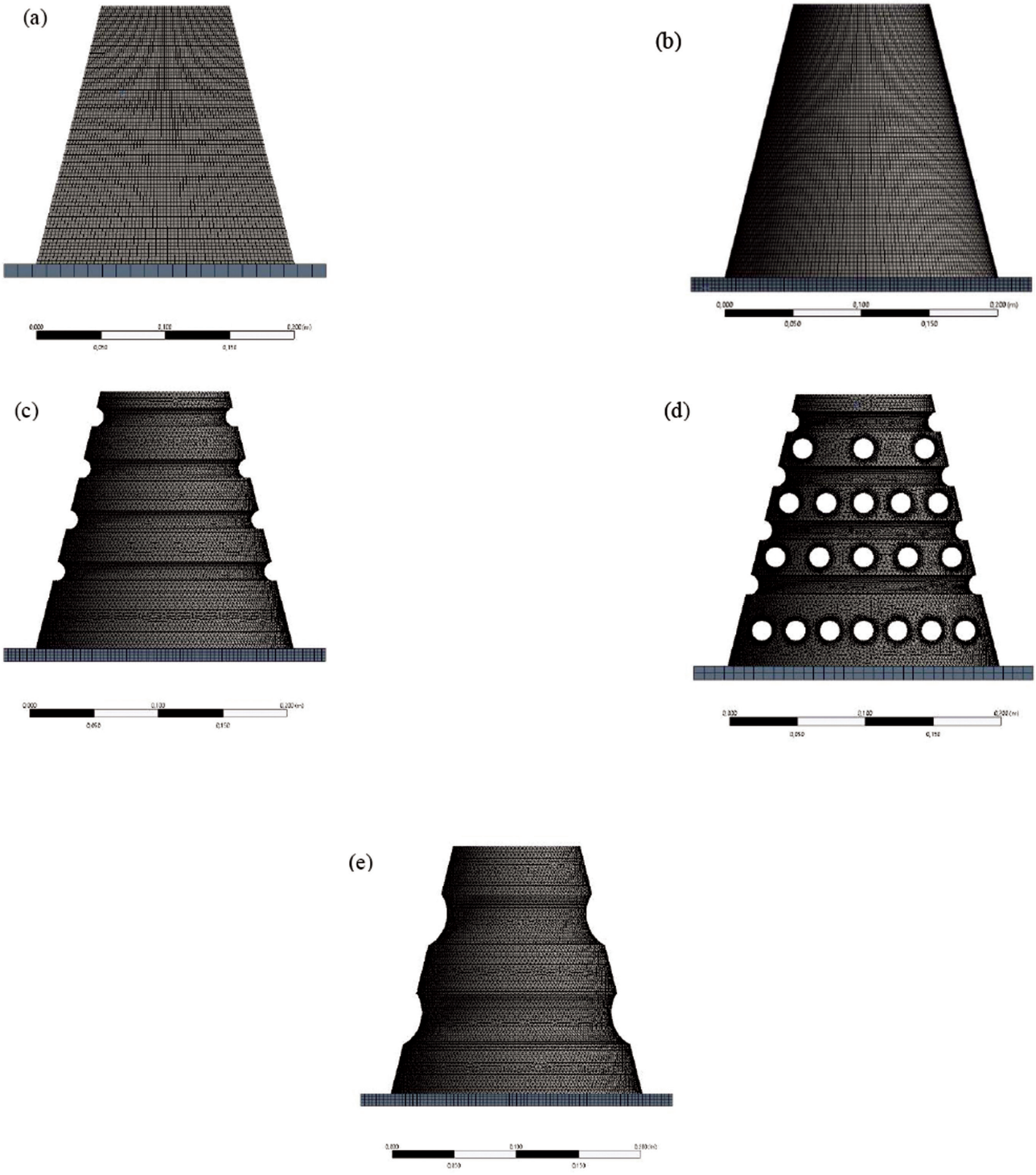

Figure 3. A detailed mesh models of impact attenuator design.

4. RESULTS AND DISCUSSIONS

Model Validation

In order to confirm the accuracy of the finite element model used in this study, an existing study from the literature was remade with the model generated in this study, and the results were compared with the original ones. Oshinibosi's study [34] was used for means of comparison. Square and circular cross-sectioned impact attenuators used in Oshinibosi's study were generated with the current model, and the results can be seen in Table 5. Also, Table 5, shows the percentage differences between the values

Table 4. Element qualities are based on the selection of element length.

Element Length [mm]	Element Quality	Skewness	Aspect Ratio	Elements	Nodes
10	0.37	0.88	3.96	10846	3796
8	0.38	0.72	3.63	13317	4663
5	0.64	0.54	2.56	32875	11144
3	0.84	0.23	1.50	91981	31012
2	0.82	0.34	1.49	276215	81438
1	0.83	0.24	1.47	2419495	544696

Table 5. Comparison of the current study and Oshinibosi's study [34].

Crash Parameters	Oshinibosi's Circular Frustum	Circular Frustum	% Difference	Oshinibosi's Square Frustum	Square Frustum	% Difference
Absorbed Energy [J]	7160.54	7347.49	2.58 %	7126.12	7182.56	0.79 %
Mass [kg]	0.52	0.56	7.41 %	0.67	0.71	5.79 %
SEA [J/kg]	13665.15	13196.16	3,49 %	10667.84	10131.69	5.16 %

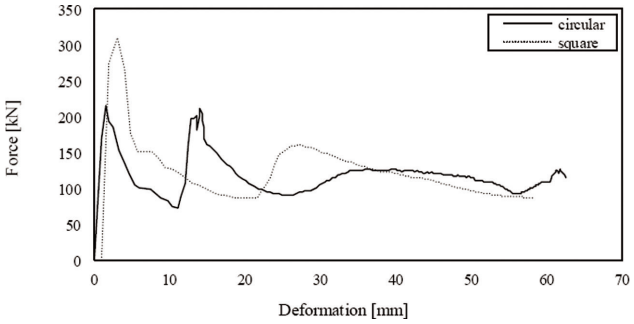

Figure 4. Comparison of impact forces with respect to deformation for circular and square cross-sectional impact attenuators.

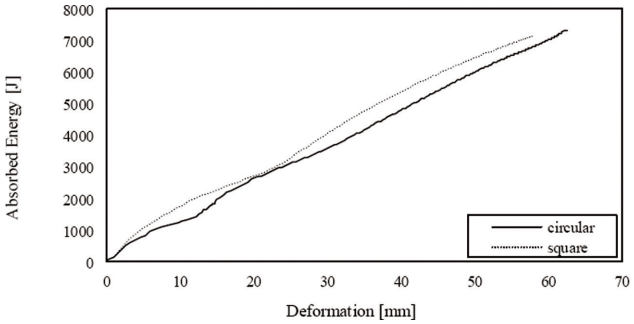

Figure 5. Comparison of absorbed energy with respect to deformation for circular and square cross-sectional impact attenuators.

between Oshinibosi's and the current study. Accordingly, the differences between original and remade models were calculated. Consequently, it was proven that the current model is working and providing accurate results as intended.

After the validation, both square and circular cross-sectioned impact attenuators are then simulated using the material AA6061-T6. The impact force difference between circular design and square design's graphical expression is shown in Figure 4 and energy absorption differences are shown in Figure 5. As shown in Table 6, the comparison of the impact attenuators shows that the circular cross-section design undergoes more amount of deformation than the square cross-section design, resulting in more efficient energy absorption. Also, the impact force efficiency of the circular cross-section impact attenuator is higher than the square-section impact attenuator which is desirable in this type of application. Therefore, the circular cross-sectioned impact attenuator has been chosen as the main geometry for optimization studies.

First Optimization

In the first optimization study, the results obtained by changing the thickness of the circular cross-sectioned impact attenuators were analyzed. In this optimization case, all models satisfy the energy absorption requirements of the regulation. However, the suitability of energy absorption alone is not sufficient. In order to improve the current design, CFE and SEA must be maximized. SEA is directly related to the mass of the impact attenuator.

The impact forces obtained as a result of the analysis are shown in Figure 6 and also, energy absorption differences between designs are shown in Figure 7. As can

Table 6. Comparison results of the analysis made according to the shape of the cross-section areas of impact attenuators.

Crash Parameters	Circular	Square
Peak Force [kN]	215.58	309.55
CFE [-]	0.54	0.34
Deformation [mm]	62.55	58.17
Absorbed Energy [J]	7347.49	7182.56
Mass [kg]	0.56	0.71
SEA [J/kg]	13196.16	10131.69

Table 7. Comparison results of the analysis made according to the thickness of impact attenuators

Crash Parameters	1 mm	2 mm	3 mm
Peak Force [kN]	114.83	215.58	359.11
CFE [-]	0.52	0.54	0.66
Deformation [mm]	132.23	62.55	30.83
Absorbed Energy [J]	7213.17	7347.49	7348.00
Mass [kg]	0.39	0.56	0.83
SEA [J/kg]	18447.99	13196.16	8879.01

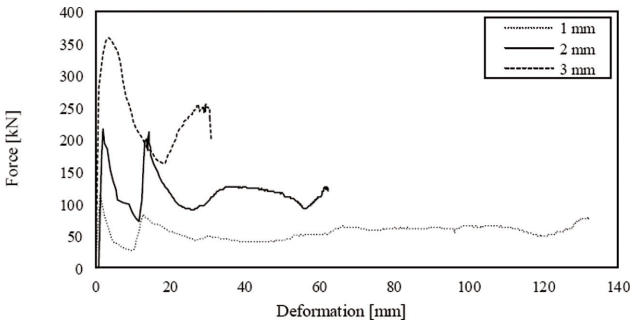

Figure 6. Comparison of impact forces with respect to deformation for 1 mm, 2 mm, and 3 mm thick impact attenuators.

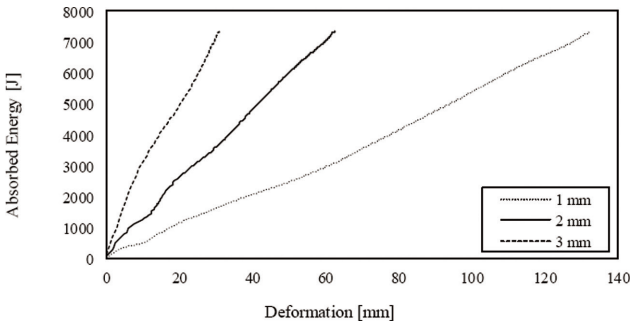

Figure 7. Comparison of absorbed energy with respect to deformation for 1 mm, 2 mm, and 3 mm thick impact attenuators.

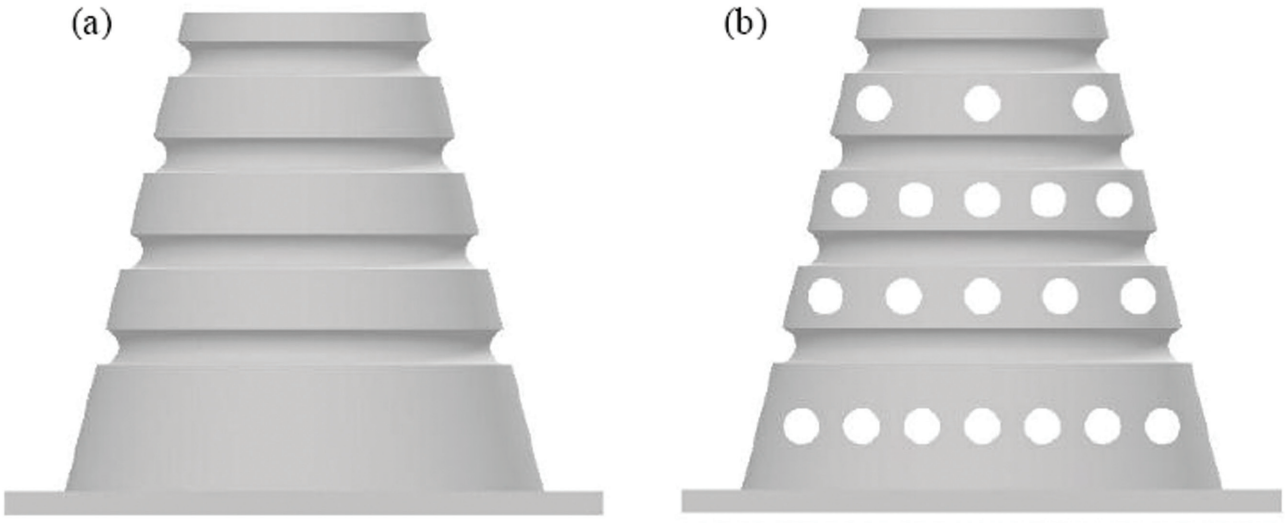

Figure 8. Impact attenuators that a) 2 mm thick with grooves and b) 2 mm thick with grooves and holes.

be seen in Table 7, the SEA value has the highest value due to the lower mass of the impact attenuator with a 1 mm thickness. However, for the model with 2 mm thickness, the CFE value is slightly higher, and the deformation length is significantly shorter when compared to the model with a thickness of 1 mm. Also, a 1 mm thick design's energy absorption is not satisfying the Formula SAE rules. For this reason, the model with 2 mm thickness was used for further optimization and improvement studies.

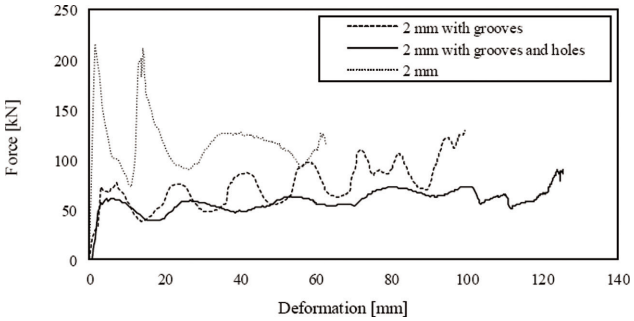

Figure 9. Comparison of impact forces with respect to deformation for the impact attenuator design with and without groves and holes.

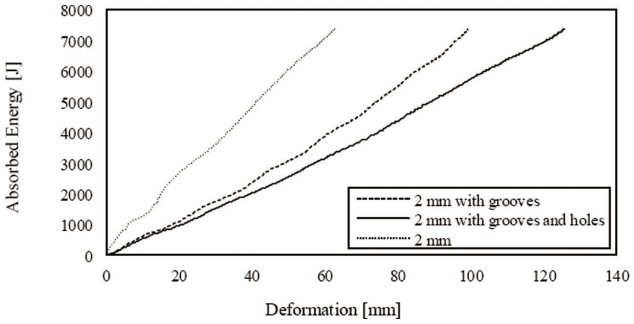

Figure 10. Comparison of absorbed energy with respect to deformation for the impact attenuator design with and without groves and holes.

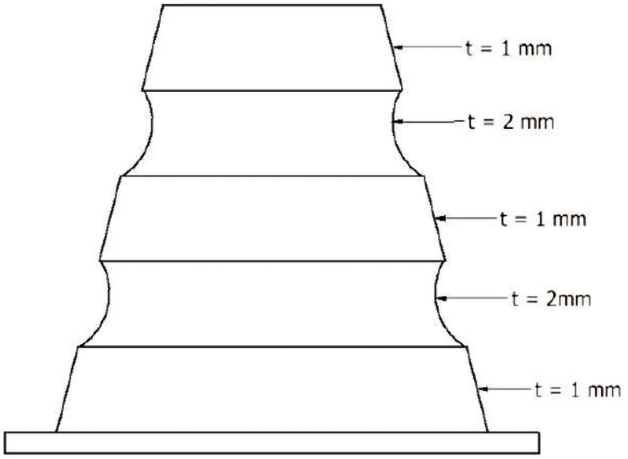

Figure 11. Details of the impact attenuator with varying wall thickness.

Table 8. Comparison of analysis results based on the presence of grooves and holes on impact attenuators.

Crash Parameters	2 mm	2 mm with grooves	2 mm with grooves and holes
Peak Force [kN]	215.58	128.63	89.78
CFE [-]	0.54	0.66	0.69
Deformation [mm]	62.55	99.36	125.69
Absorbed Energy [J]	7347.49	7350.30	7344.79
Mass [kg]	0.56	0.62	0.56
SEA [J/kg]	13196.16	11958.13	13066.46

Second Optimization

Based on the previous optimization cases, the design parameters of the impact attenuator have been determined as having a circular cross-section with a thickness of 2 mm. In the second optimization, the effect of the grooves and holes on the lateral surfaces of the impact attenuator designs was investigated. The design of the impact attenuator with grooves and with additional holes are shown in Figures 8a and 8b respectively. It is expected that the holes and grooves on the lateral surfaces increase the energy absorption rate by increasing the deformation of the impact attenuator and increase the specific energy absorption due to the decrease in mass.

Analysis results show that grooves and holes on lateral surfaces significantly increase the deformation values and decreases the impact forces as shown in Figure 9 and 10. Also, CFE was improved due to the existence of grooves and holes as shown in Table 8. However, SEA has not been improved since the mass of designs with grooves and holes on their lateral surfaces cannot be reduced. Thus, the impact attenuator's mass must be minimized to increase SEA.

Third Optimization

In the final optimization, a new impact attenuator design was tested. As a result of the observations from the previous optimizations, it was aimed to increase the deformation of the impact attenuator in the collision, hence increase the specific energy absorption. As can be seen in Figure 11, it was aimed to increase the deformation by reducing the wall thickness of the parts outside the grooves on the impact attenuator.

As can be seen in the impact attenuator with varying wall thickness has resulted in more efficient values than all the other designs made within the scope of this study. Due to the increase in the deformation value shown in Table 13, there was a decrease in the values of the impact force. It can be seen in Table 12 that the impact forces decreased substantially for the design with varying thicknesses. When all designs are compared in Table 9, the design with varying wall thickness has the highest deformation, CFE, and SEA values. Also, the impact forces are significantly lower. With this design, global buckling was avoided, and local buckling was achieved as shown in Figure 14. Consequently, the design with grooves and varying thicknesses was determined to be the most efficient and optimized design among the other designs considered in this study.

Table 9. Comparison of the analysis results of all impact attenuator designs including varying wall thickness cases.

Crash Parameters	2 mm	2 mm with grooves	2 mm with grooves and holes	varying thickness with grooves
Peak Force [kN]	215.58	128.63	89.78	75.49
CFE [-]	0.54	0.66	0.69	0.78
Deformation [mm]	62.55	99.36	125.69	151.66
Absorbed Energy [J]	7347.49	7350.30	7344.79	7355.75
Mass [kg]	0.56	0.62	0.56	0.44
SEA [J/kg]	13196.16	11958.13	13066.46	16830.07

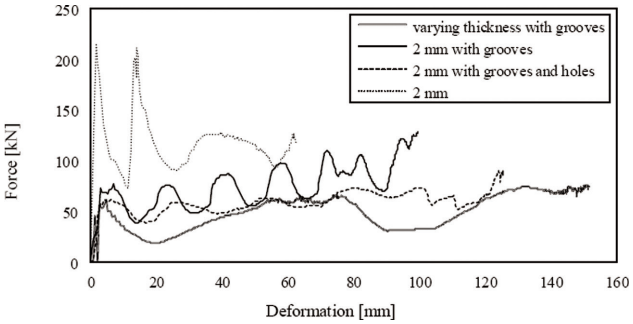

Figure 12. Comparison of the impact forces with respect to deformation for all impact attenuator designs including varying wall thickness cases.

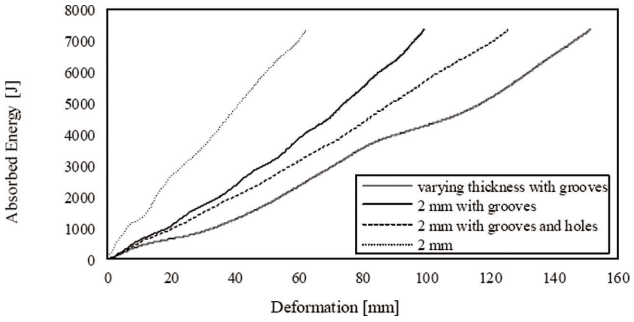

Figure 13. Comparison of the absorbed energy with respect to deformation for all impact attenuator designs including varying wall thickness cases.

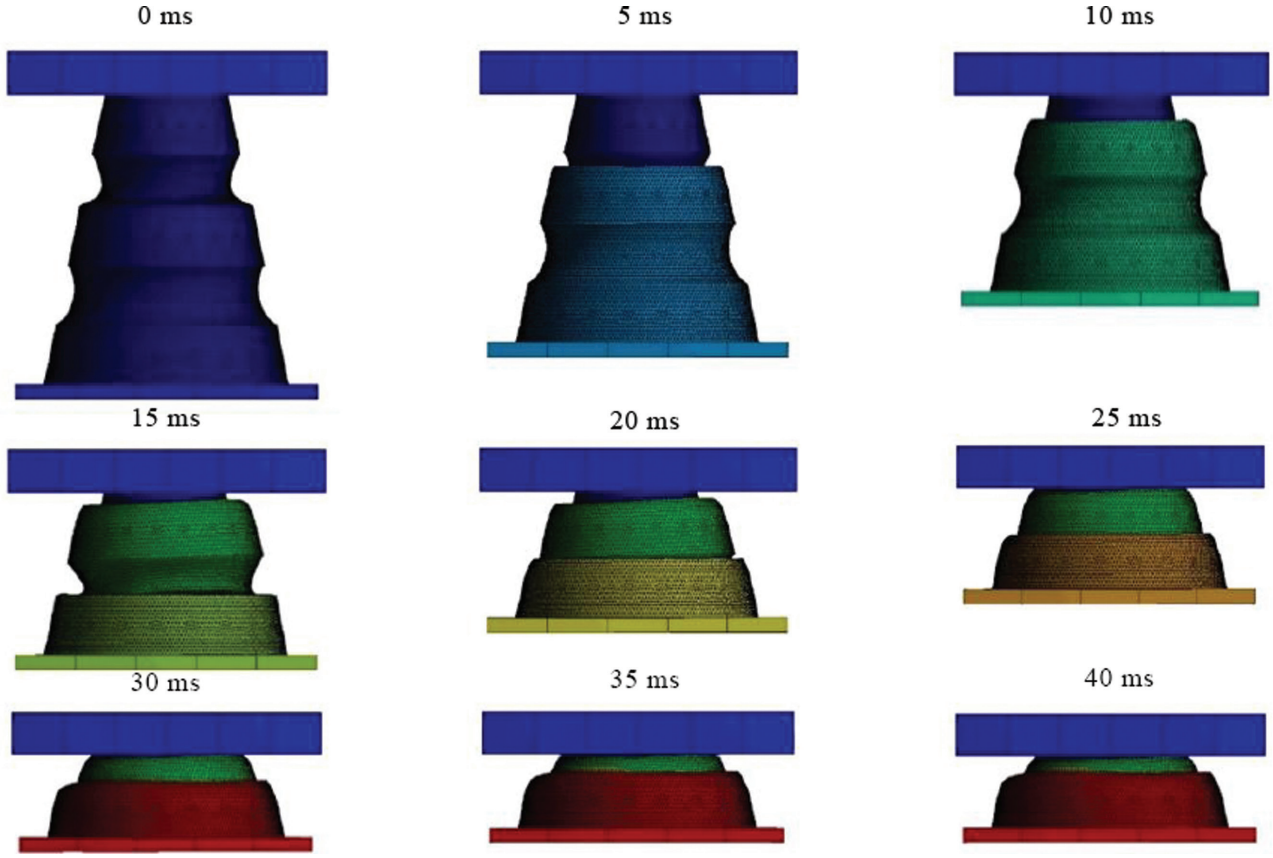

Figure 14. Deformation of the design with varying wall thickness over time.

5. CONCLUSION

In this study, impact attenuators with different geometrical properties designed in accordance with Formula SAE rules were subjected to collision analysis. The analysis was carried out by means of varying thickness, cross-sectional shape, and optimization of grooves and holes in designs.

From the collision analysis, the following conclusions can be made;

- Circular cross-section design has higher CFE and deformation values compared to square cross-sectional geometries.
- Sharp corners in the absorber geometry need to be avoided to not to reduce the crash forces and to not experience global buckling.
- Grooves on lateral surfaces of the impact attenuator increase the deformation and the crash force efficiency.
- Holes on the design increase both crash force efficiency and specific energy absorption due to reduced mass.
- By determining the critical crumple zones in the design, more efficient absorbers can be designed by reducing the wall thickness in particular regions of the model.

In conclusion, the design with varying wall thickness was found to be the most efficient design in terms of energy absorption performance and specific energy absorption. 64.99 % reduction on maximum impact force was observed between the first design and the final design with varying thickness. Also, an increase of 58.76 % deformation and 30.77 % crash force efficiency was observed. As a result, the impact attenuator with varying thickness with grooves satisfied the requirements expected from a Formula SAE type racing car and therefore it was selected for use in future competitions.

AUTHORSHIP CONTRIBUTIONS

Authors equally contributed to this work.

DATA AVAILABILITY STATEMENT

The authors confirm that the data that supports the findings of this study are available within the article. Raw data that support the finding of this study are available from the corresponding author, upon reasonable request.

CONFLICT OF INTEREST

The author declared no potential conflicts of interest with respect to the research, authorship, and/or publication of this article.

ETHICS

There are no ethical issues with the publication of this manuscript.

REFERENCES

[1] G.I. Association. Accident Statistics and Potential Driver Assistance Systems, 2020. Available at: https://m.udv.de/en/publications/compact-accident-research/accident-statistics-and-potential-driver-assistance-systems Accessed on Jun 20, 2020.

[2] Belingardi G, Chiandussi G. Vehicle crashworthiness design—general principles and potentialities of composite material structures, Impact engineering of composite structures. New York: Springer; 2011:193–264. [CrossRef]

[3] Tarlochan F, Ramesh S, Harpreet S. Advanced composite sandwich structure design for energy absorption applications: blast protection and crashworthiness. Compos B Eng 2012;43:2198–2208. [CrossRef]

[4] SAE. Formula SAE Rules, 2020. Available at: http://fsaeonline.com/cdsweb/gen/DownloadDocument.aspx?DocumentID=d9fa3638-59f8-411c-a487-e27abc2d9022. Accessed on Jun 20, 2020.

[5] Alghamdi AAA. Folding-crumpling of thin-walled aluminium frusta. Int J Crashworthiness 2002;7:67–78. [CrossRef]

[6] Marzbanrad J, Mehdikhanlo M, Saeedi Pour A. An energy absorption comparison of square, circular, and elliptic steel and aluminum tubes under impact loading. Turkish J Eng Environ Sci 2009;33:159–66.

[7] Langseth M, Hopperstad O. Static and dynamic axial crushing of square thin-walled aluminium extrusions. Int J Impact Eng 1996;18:949–968. [CrossRef]

[8] Marzbanrad J, Alijanpour M, Kiasat MS. Design and analysis of an automotive bumper beam in low-speed frontal crashes. Thin-Walled Struct 2009;47:902–911. [CrossRef]

[9] Tanlak N, Sonmez FO, Senaltun M. Shape optimization of bumper beams under high-velocity impact loads. Eng Struct 2015;95:49–60. [CrossRef]

[10] Carney III JF, Pothen S. Energy dissipation in braced cylindrical shells. Int J Mech Sci 1988;30:203–216. [CrossRef]

[11] Alexande JM. An approximate analysis of the collapse of thin cylindrical shells under axial loading. Q J Mech Appl Math 1960;13:10–15. [CrossRef]

[12] Reid S, Austin C, Smith R. Tubular rings as impact energy absorbers. Amsterdam: Elsevier lsevier Applied Science Publication; 1984:555–563.

[13] Nannucci P, Marshall N, Nurick G. A computational investigation of the progressive buckling of square tubes with geometric imperfections. Third Asia-Pacific conference on Shock and Impact Loads on Structures; 1999. p. 24–26.

[14] Singacee AA, El-Sobky H. Behaviour of axially crushed corrugated tubes. Int J Mech Sci 1997;39:249–268. [CrossRef]

[15] Wierzbicki T, Abramowicz W. On the crushing mechanics of thin-walled structures. J Appl Mech 1983,50:727–734. [CrossRef]
[16] Mamalis AG, Johnson W. The quasi-static crumpling of thin-walled circular cylinders and frusta under axial compression. Int J Mech Sci 1983;25:713–732. [CrossRef]
[17] Harris JA, Adams RD. An assessment of the impact performance of bonded joints for use in high energy absorbing structures. Proceedings of the Institution of Mechanical Engineers, Part C. J Mech Eng Sci 1985;199:121–131. [CrossRef]
[18] Wierbicki T. Crushing analysis of metal honeycombs. Int J Impact Eng 1983;1:157–174. [CrossRef]
[19] Corbett G, Reid S. Local loading of simply-supported steel—grout sandwich plates. Int J Impact Eng 1993;13:443–461. [CrossRef]
[20] Stangl P, Meguid S. Experimental and theoretical evaluation of a novel shock absorber for an electrically powered vehicle. Int J Impact Eng 1991;11:41–59. [CrossRef]
[21] White MD, Jones N. Experimental quasi-static axial crushing of top-hat and double-hat thin-walled sections. Int J Mech Sci 1999;41:179–208. [CrossRef]
[22] Boria S, Pettinari S, Giannoni F. Theoretical analysis on the collapse mechanisms of thin-walled composite tubes. Compos Struct 2013;103:43–49. [CrossRef]
[23] Witterman W. Improved vehicle crashworthiness design by control of the energy absorption for different collision situations. [Doctorial Thesis]. Eindhoven, Netherlands: University of Technology, Automotive Engineering and Product Design Technology; 1999.
[24] Design of the impact attenuator for a formula student racing car: numerical simulation of the impact crash test. J Serb Soc Comput Mech 2010;4:52–65.
[25] Jensen O, Langseth OS, Hopperstad OS. Transition between progressive and global buckling of aluminium extrusions. WIT Transactions on The Built Environment 63, 2002. Available at: https://www.witpress.com/Secure/elibrary/papers/SU02/SU02026FU.pdf Accessed on May 20, 2022.
[26] Karagiozova D, Jones N. On the mechanics of the global bending collapse of circular tubes under dynamic axial load—Dynamic buckling transition. Int J Impact Eng 2008;35:397–424. [CrossRef]
[27] Zhang XW, Su H, Yu TX. Energy absorption of an axially crushed square tube with a buckling initiator. Int J Impact Eng 2009;36:402–417. [CrossRef]
[28] Taher ST, Mahdi E, Mokhtar AS, Magid DL, Ahmadun FR, Arora PR. A new composite energy absorbing system for aircraft and helicopter. Compos Struct 2006;75:14–23. [CrossRef]
[29] Ozguc O. The assessment of impact damage caused by dropped objects on floating offshore structures. Proc Inst Mech Eng M J Eng Marit Environ 2021;235:491–510. [CrossRef]
[30] Çelik Aİ, Köse MM, Akgül T, Alpay AC. Directional-deformation analysis of cylindrical steel water tanks subjected to el-centro earthquake loading. Sigma J Eng Nat Sci 2018;36:1033–1046.
[31] Yavuz H. Cylindro-conical mild steel projectile impact on e-glass fiber reinforced laminated composite plate including delamination analysis. Eur Mech Sci 2021;5:21–27. [CrossRef]
[32] Yang DY, Jung DW, Song IS, Yoo DJ, Lee JH. Comparative investigation into implicit, explicit, and iterative implicit/explicit schemes for the simulation of sheet-metal forming processes. J Mater Process Technol 1995;50:39–53. [CrossRef]
[33] Rikards R, Chate A, Ozolinsh O. Analysis for buckling and vibrations of composite stiffened shells and plates. Compos Struct 2001;51:361–370. [CrossRef]
[34] Oshinibosi A. Chassis and impact attenuator design for formula student race car. Univesity of Leeds School of Mechanical Engineering; 2012. p. 1–81. Available at: https://altairuniversity.com/wp-content/uploads/2014/04/Ahmed-Oshinibosi.pdf Accessed on May 20, 2022.
[35] Lesuer DR, Kay HJ, Lebland MM. Modeling large-strain, high-rate deformation in metals. Lawrence Livermore National Lab. California, USA; 2001. Available at: https://www.osti.gov/servlets/purl/15005327 Accessed on May 20, 2022.
[36] A.M.A. ANSYS, Theory Reference, Release 17.0. Canonsburg, PA: Ansys Inc; 2016.